KSME

Springer

Journal of Mechanical Science and Technology 36 (10) 2022

Original Article
DOI 10.1007/s12206-022-0936-6

Keywords:
· Adaptive impedance control
· Contact force tracking
· Industrial robot
· Unknown environment

Correspondence to:
Chungang Zhuang
cgzhuang@sjtu.edu.cn

Citation:
Shen, Y., Lu, Y., Zhuang, C. (2022). A fuzzy-based impedance control for force tracking in unknown environment. Journal of Mechanical Science and Technology 36 (10) (2022) ?~?.
http://doi.org/10.1007/s12206-022-0936-6

Received December 28th, 2021
Revised June 11th, 2022
Accepted June 28th, 2022

† Recommended by Editor
Ja Choon Koo

A fuzzy-based impedance control for force tracking in unknown environment

Yichao Shen, Yan Lu and Chungang Zhuang

School of Mechanical Engineering, Shanghai Jiao Tong University, Shanghai 200240, China

Abstract Industrial manufacturing operations, such as grinding and polishing, are characterized by relatively constant contact force. In this article, a fuzzy-based adaptive impedance is proposed, which can grind or polish workpieces of different materials with constant contact force. The environmental parameters are estimated by iterative calculation with recursive least squares (RLS). The impedance parameters, such as damping and stiffness, are taken as the outputs of the fuzzy controller. The proposed force controller can track the desired force without the prior knowledge of the environment information. Experiments are conducted in finishing tasks using the self-developed industrial robot to verify the adaptive impedance control. The environmental parameters are instantly estimated for the following adjustment of the impedance parameters, and the real time contact force shows that the adaptive fuzzy logic impedance controller can achieve better performance with the oscillation below 2 N as the machining surface of the workpiece is not predefined.

1. Introduction

With the fast development of the robot technology, robotic research has achieved numerous advances in the industrial manufacturing industry. The tasks which need interactions with the external environment are challenging for the industrial robots. Also, the human operators can hardly compensate accurately for the subtle position or the force error.

To handle the above-mentioned issues, the adaptive force control is necessarily in robot manufacturing field with the desired force while the desired trajectories are followed [1]. Seraji and Colbaugh [2] proposed a trajectory correction scheme, and an adaptive technology was used to estimate the environmental stiffness and adjust the controller gain to compensate the known environmental stiffness. The force tracking was obtained by using the extended Kalman filter in Ref. [3] and the control gain was analytically defined based on the estimation of the stiffness. The position-based impedance controller was studied in Ref. [4] to track the desired force by using the adaptive environmental estimated parameters. In addition, the variable impedance control is also a good choice. The basic principle of the variable impedance control is to adjust the impedance parameters according to the force feedback information. A model free reinforcement learning method was proposed in Ref. [5], which can learn the variable impedance control of robot system for optimal control. Kronander and Billard [6] presented an online, incremental algorithm for learning the variable stiffness.

In recent years, scholars have done a lot of theoretical and practical researches on the noise and error of the robot impedance control under the unknown properties of the external environment and position [7, 8]. Na [9] proposed a new impedance force control model of a haptic device for teleoperation. Zhu and Barth [10] used the principle of the sliding mode control to design a control algorithm for the end contact force of the manipulator and optimized the constant contact force to achieve a stable effect. Panwar and Sukavanam [11] studied the state equation of the robot, they built the control framework of the robot by the optimal theory and the synovial control algorithm. At the same time, they compensated the dynamic parameters using the network, and improved the identification accuracy and the stability of the control algorithm. Cao et al. [12] proposed the adaptive hybrid impedance control algorithm for the contact force

tracking in uncertain environments.

In a hybrid position/force controller for surface finishing, the position is generally regulated along the surface, while the force is usually controlled in normal directions. For the position control in the robot machining, the hybrid control requires accurate knowledge of surface geometry to yield a good surface finish. Surdilovic [13] utilized CAD/CAM software to generate paths for milling and grinding very hard materials like Inconel, and proposed a combination of force and feed control for polishing the hard materials. Bonilla et al. [14] performed path tracking maneuvers using the impedance control on industrial robots. A comprehensive overview related to the robot force control can be found in Ref. [15]. The force control strategies and the hybrid position/force control of robotic manipulators have been extensively deployed for finishing processes including deburring, polishing and grinding. Nagata et al. [16] has made many achievements related to the grinding and polishing algorithms. The control algorithm suitable for surface constant force tracking was applied to the actual grinding and polishing processing, and the force/position hybrid control algorithm was adopted to ensure the uniformity of grinding quantity and machining accuracy. Domroes et al. [17] applied the force control module in controller to grind and polish, and studied and analyzed the process parameters by comparing the effects under the force and position control. In a pioneering work, Kazerooni et al. [18] developed and implemented the impedance control methodology for deburring and grinding. Later, Wang et al. [19] developed an adaptive framework based on the impedance control in which the cutting force and the feed rate were adjusted automatically to obtain better quality, in which a model was developed to predict the cutting force.

The fuzzy logic control with expert expertise has been integrated into the robot controller with the development of artificial intelligence algorithms. The hybrid position/force control based on the fuzzy control was proposed for obtaining the desired chamfer depth by Hsu and Fu [20]. A fuzzy-PI controller was integrated into the variable impedance algorithm, which was applied to the robot trimming system [21]. Li et al. [22] proposed a fuzzy adaptive admittance control algorithm and applied it to the UR5 manipulator, which achieved better performance in the uncertain contact environment.

In the above research, the input of the fuzzy logic control is the force tracking error and its first derivative. When the derivative of the force tracking error is prone to a peak value, it will cause input saturation of the fuzzy logic controller, alter the controller output resolution, and reduce the force control precision. Furthermore, the preceding technique employs the fuzzy logic control to alter the impedance parameters without taking into account the environmental information. Thus, previous research considered the significant effect of the environmental conditions on force control performance.

Recently, the neutrosophic logic/statistics [23-28] were proposed to study the fuzziness and uncertainty factors in natural data which can be regarded as an extension of the fuzzy logic. In the complex scenarios, the neutrosophic logic has better discrimination than the fuzzy logic. Some works in Refs. [23-28] have made lots of achievements in neutrosophic logic/statistics. The existing environmental parameter estimation method [29] models the external environment in contact with the robot as a system composed of stiffness and damping, and the complex nonlinear nature of the environment and some other influencing factors are ignored. Although this method loses certain accuracy, it has been proved to be effective in practice. In this article, due to the simplification of the environmental model, there are relatively few influencing factors and parameters for the proposed fuzzy-based impedance control. When more complex models and factors are considered, the neutrosophic logic/statistics [23-28] can be adopted to optimize the adaptive impedance control algorithm.

In this article, an adaptive impedance control method, that uses the fuzzy control and applies environmental parameter estimation, is proposed to refine the force control performance for robot machining. The main contributions are listed as follows:

The adaptive impedance control model is proposed based on the fuzzy control. The fuzzy-based controller adjusts the stiffness and the damping parameters, which effectively improves the response speed and the stability of the control law.

In the fuzzy control model, the fuzzy architecture is constructed with the contact force and the environmental parameters, which are estimated by the RLS, as inputs. This model can keep constant force tracking in the unknown environment.

Numerical simulations and experiments are conducted to verify the effectiveness of the proposed method. The constant force tracking error is reduced, which shows the feasibility of this method in practical application.

This article uses the fuzzy logic to improve the control performance of contact force between robot and environment. The proposed method can be potentially applied to industrial scenes where robots are in contact with the external environment, such as robot assembling, robot machining and human-robot cooperation. Especially in human-robot cooperation, the performance of the contact force control will affect people's life safety.

2. Preliminaries

In this section, the interaction model between robot and environment is introduced as follows. The dynamics model of a robot manipulator can be written as follows:

$$I(x)\ddot{x} + C(x,\dot{x})\dot{x} + g(x) = u + f_e \tag{1}$$

where x is the location of the end-effector's manipulator. $I(x)$ and $C(x,\dot{x}) \in \mathbb{R}^{N\times N}$ are the inertia and the Coriolis/centrifugal matrix, $g(x) \in \mathbb{R}^{N\times 1}$ is the gravitational vector. Moreover, u and $f_e(x) \in \mathbb{R}^{N\times 1}$ are the control inputs, and the external force vector at the end-effector [30]. The environment can be considered as a second order mass-spring-damper system. How-

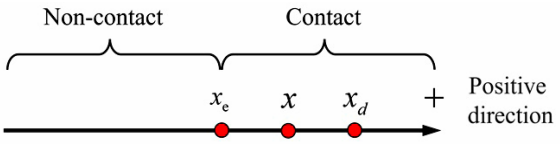

Fig. 1. The specified positive direction.

ever, in this article, for the sake of simplicity, the environment is modeled by a single spring:

$$\begin{cases} f_e = 0, \ x \le x_e \\ f_e = k_e\left(x - x_e\right), \ x > x_e \end{cases} \tag{2}$$

where x_e is the location of the environment, x is the end-effector's location of the manipulator, k_e is the stiffness parameter of environment. The specified positive direction is shown in the Fig. 1.

3. Proposed method

To handle the issue of the undefined machining workpiece's surface, a new adaptive impedance control algorithm is proposed to enhance the interaction control between the robot and the unknown changing environment. This method can improve the force tracking performance. Compared with the previous literature [12, 30], the environmental parameter estimation and the impedance parameter tuning based on the fuzzy logic are integrated to the framework of the impedance control to achieve the adaptive force control in this article.

The first three parts of Sec. 3 introduce the submodules of the proposed method. The impedance control is presented at first. Then, the parameters of the unknown variable environment are estimated. Sec. 3.4 gives the proposed framework of the adaptive fuzzy impedance control, which is the main work of this article. In addition, the adjustment rules of the adaptive impedance control are given.

3.1 Impedance control

The robot impedance control model in task space can be written as follows:

$$\begin{aligned} &\mathbf{M}\left[\ddot{\mathbf{X}}(t) - \ddot{\mathbf{X}}_d(t)\right] + \mathbf{B}\left[\dot{\mathbf{X}}(t) - \dot{\mathbf{X}}_d(t)\right] \\ &\qquad + \mathbf{K}\left[\mathbf{X}(t) - \mathbf{X}_d(t)\right] = \mathbf{E}(t), \end{aligned} \tag{3}$$

$$\mathbf{E}(t) = \mathbf{F}_d(t) - \mathbf{F}_e(t) \tag{4}$$

where $\mathbf{X}(t)$, $\mathbf{X}_d(t) \in \mathbb{R}^{N\times 1}$ are the command and the desired positions of the end-effector's manipulator. $\mathbf{M}, \mathbf{B}, \mathbf{K} \in \mathbb{R}^{N\times N}$ are the inertia, damping and stiffness matrix, $\mathbf{F}_d(t)$ is the desired external force [31].

When the contact between robot and environment reaches a steady state, $\ddot{\mathbf{X}}_d$, $\ddot{\mathbf{X}}$, $\dot{\mathbf{X}}_d$ and $\dot{\mathbf{X}}$ are all equal to zero. substituting the above conditions into Eq. (4), and considering the case of single dimension:

$$k_d\left(x_d - x\right) = k_e\left(x - x_e\right) - f_d. \tag{5}$$

Then, after rearrangement:

$$x = \frac{k_d}{k_d + k_e}x_d + \frac{k_e}{k_d + k_e}x_e + \frac{f_d}{k_d + k_e}. \tag{6}$$

Substituting Eq. (6) into the definition of force tracking error Eq. (4) yields:

$$e_{ss} = k_{eq}\left(x_e - x_d + \frac{f_d}{k_e}\right) \tag{7}$$

where k_d is the stiffness parameter of the impedance controller, k_e is the stiffness parameter of environment, k_{eq} is the equivalent stiffness with $k_{eq} = k_d k_e / \left(k_d + k_e\right)$.

Therefore, it can be deduced that when the system is stable, the contact force is:

$$\begin{aligned} f_{ss} &= f_r - e_{ss} \\ &= k_{eq}\left(\frac{k_d + k_e}{k_d k_e}f_r - x_e + x_d - \frac{k_d}{k_d k_e}f_r\right) \\ &= k_{eq}\left(\frac{1}{k_d}f_d - x_e + x_d\right). \end{aligned} \tag{8}$$

In order to make the error of contact force tend to zero when the system is stable, the desired trajectory needs to be satisfied. Therefore, the environment location x_e and the ambient stiffness k_e need to be known to calculate the desired trajectory x_d. However, in the actual application scenario, the environment location x_e and stiffness k_e are difficult to be obtained, so the deviations of x_e and k_e between the real value and the estimated value are considered. The deviation of the environmental position is defined as $\Delta x_e = x_e - \hat{x}_e$. The deviation of the environmental stiffness is given as $\Delta k_e = k_e - \hat{k}_e$. At this time, the desired trajectory represented by the estimated value of the environmental parameters is: $x_d = \hat{x}_e + f_d / \hat{k}_e$. Then the steady-state error of the force calculated from the estimated value of the environmental parameters is written by:

$$e_{ss} = \frac{k_d}{k_d + k_e}\left(k_e \Delta x_e - \frac{\Delta k_e}{\hat{k}_e}f_d\right). \tag{9}$$

When the deviation Δx_e of the environmental position is small, if the environmental stiffness k_e is large enough, the steady-state error of the generated force will also be large. Therefore, to control the magnitude of the steady-state error, it is necessary to estimate the environmental stiffness, position, and other information first. The on-line estimation algorithm of the external environment is very necessary, and the steady-

state error can be controlled by the algorithm.

3.2 RLS algorithm for estimation of environment

Consider the external environment model as the mass spring damper system:

$$F_e = B_e\dot{x} + K_e\left(x - x_e\right). \tag{10}$$

For $\delta x = x - x_e$, the external environment x_e will not change over time, therefore, $\dot{x}_e$ = 0, the above formula can be written as:

$$F_e = B_e\delta\dot{x} + K_e\delta x. \tag{11}$$

The discrete-time counterpart is given as:

$$F_e = \left[B_e\left(\frac{2}{T}\right)\left(\frac{1-z^{-1}}{1+z^{-1}}\right) + K_e\right]\delta x \tag{12}$$

where *T* is the sampling period. The equation can be expanded into a polynomial of *z*. By recognizing that z^{-1} represents the offset of one step in the time domain, let k represents the time step index, and the corresponding difference equation is:

$$\begin{aligned} &F_{e[k]} + F_{e[k-1]} \\ &= \left[B_e\left(\frac{2}{T}\right) + K_e\right]\delta x_{[k]} + \left[K_e - B_e\left(\frac{2}{T}\right)\right]\delta x_{[k-1]} \\ &= \alpha\delta x_{[k]} + \beta\delta x_{[k-1]}. \end{aligned} \tag{13}$$

The above formula can be expressed as: $y_{[k]} = \phi_{[k]}^T\theta_{[k]}$, with $y_{[k]} = F_{e[k]} + F_{e[k-1]}$, $\phi_{[k]} = \left[x_{[k]} - x_e \quad x_{[k-1]} - x_e\right]^T$, and $\theta_{[k]} = \left[\alpha \quad \beta\right]^T$.

The RLS solution for $\theta_{[k]}$ takes the following form:

$$\theta_{[k]} = \theta_{[k-1]} + L_{[k]}\left(y_{[k]} - \phi_{[k]}^T\theta_{[k-1]}\right), \tag{14}$$

$$L_{[k]} = \frac{P_{[k-1]}\phi_{[k]}}{\lambda + \phi_{[k]}^T P_{[k-1]}\phi_{[k]}}, \tag{15}$$

$$P_{[k]} = \frac{1}{\lambda}\left(P_{[k-1]} - \frac{P_{[k-1]}\phi_{[k]}\phi_{[k]}^T P_{[k-1]}}{\lambda + \phi_{[k]}^T P_{[k-1]}\phi_{[k]}}\right) \tag{16}$$

where $L_{[k]}$ is the coefficient of the adaptive gain in the time estimation algorithm, the initial guess for the adaptation gain matrix *P* and the weighting factor $\lambda(0 \le \lambda \le 1)$ must be specified by the user. The value of the weighting factor will determine the proportion of the data collected before the time *k*. When the value of λ is reduced, the influence of the previously collected data on the covariance matrix is smaller and more sensitive to the latest data. Therefore, when the external environment does not change or the change of environmental parameters is very small, the value of forgetting factor should be slightly less than 1.

Under this selection condition, the previously collected data can provide reference value for the estimated environmental parameters. If the weighting factor is large, it can increase the robustness to the noise brought by the external environment. At the same time, in the case of variable environmental stiffness, the first collected data will be expected to have less impact on the estimated value of environmental parameters. Therefore, in this case, it is necessary to select smaller weighting factor λ to ensure that the algorithm meets the ability of variable parameter calculation:

$$\lambda_{[k]} = \lambda_{\min} + \left(\lambda_{\max} + \lambda_{\min}\right)e^{-\beta e_{[k]}^T e_{[k]}} \tag{17}$$

where $\lambda_{\min}$ and $\lambda_{\max}$, respectively, represent the minimum and maximum values of the weighting factor in the selected range, and β is the parameter to adjust the response speed and the error of the system. Therefore, when the transformation of the external environment is small or basically unchanged, the estimation error is also small. At this time, the maximum value of the forgetting factor should be selected to effectively suppress the interference of external noise on the estimated value. On the contrary, when the external environment constantly changes, the estimation error will also become larger, and the minimum value of the forgetting factor should be selected, it can reduce the impact of the previously collected data on the estimated value, improve the ability of real-time change of the estimated value, and increase its response speed.

Once $\theta_{[k]}$ has been calculated (and subsequently α, β), the desired parameter estimated at the *k*th sample period can be recovered by using:

$$\begin{cases} K_e = \left(\alpha + \beta\right)/2 \\ B_e = T\left(\alpha - \beta\right)/4 \end{cases}. \tag{18}$$

3.3 Unknown variable environment

Due to the unknown environmental information, it is difficult to propose the desired trajectory x_d. In this work, two main interactive environment information are not available, including the location and stiffness of the environment. In fact, it can be assumed that the environment changes with time. Therefore, the robot should be able to maintain contact with the variable environment. Thus, the one-dimension interaction force is rewritten as:

$$m_d\ddot{e}_x + b_d\dot{e}_x + k_d e_x = f_e - f_d \tag{19}$$

where $e_x = x - x_e$ is expressed as the difference between the end position of the manipulator and the environment position, f_e is the interaction force at the end-effector with the environment, f_d is the desired force [19].

When the desired contact force is zero and the end of the

manipulator is just in contact with the environment, it means that Δf_{ss} = 0 when $e_x = x - x_e = 0$. In this case, the external environment with arbitrary stiffness can meet the requirements. However, when the desired contact force is $f_d \neq 0$ and the robot contacts the surface of the environment, it can be observed that $x \neq x_e$ and $\Delta f_{ss} \neq 0$. In order to make the force error at the end of the manipulator in contact with the external environment tend to zero, set k_d = 0, yields:

$$\Delta f = f_e - f_d = m_d \ddot{e}_x + b_d \dot{e}_x . \tag{20}$$

After simplifying, it yields:

$$m_d \left(\ddot{x} - \ddot{x}_e \right) + b_d \left(\dot{x} - \dot{x}_e \right) = f_e - f_d . \tag{21}$$

For arbitrary environmental stiffness k_d, the appropriate parameters m_d and b_d can be selected to make the above formula set up. Therefore, in impedance control, when the stiffness parameter k_d = 0, the error of force at the final stability is always 0.

When the external environment is a plane, $\ddot{x}_e = \dot{x}_e = 0$, the equation can be simplified as:

$$m_d \ddot{x} + b_d \dot{x} = f_e - f_d . \tag{22}$$

Currently, the system is stable and Δf_{ss} = 0.

When the external environment is a complex surface, x_e changes over time with $\dot{x} \neq 0$ and $\ddot{x}_e \neq 0$. Therefore, the location of the external environment x_e needs to be estimated. It can be assumed that the estimated value of the location of the external environment is $\hat{x}_e$ and the uncertainty of the environment position is δx_e, which yields $\hat{x}_e = x_e - \delta x_e$. Currently, the trajectory error estimation $\hat{e}_x = x - \hat{x}_e$ is rewrites as $\hat{e}_x = e_x + \delta x_e$. Also, the uncertainty of the interaction force is δf for the unknown stiffness of the environment with $e_f = f_e - f_d$ and $\hat{e}_f = e_f + \delta f$. The equation of impedance control can be simplified as:

$$m_d \left(\ddot{e}_x + \delta \ddot{x}_e \right) + b_d \left(\dot{e}_x + \delta \dot{x}_e \right) = e_f + \delta f . \tag{23}$$

By adjusting the damping parameters b_d in the impedance control in real time, the steady-state error of the final contact force tends to zero [32].

3.4 Adaptive fuzzy impedance control

The adaptive fuzzy impedance control algorithm in this section is based on the preceding three portions. The adaptive fuzzy impedance control schematic is shown in Fig. 2. In the proposed method, the environmental parameter estimation and the impedance parameter tuning based on the fuzzy logic are added to the framework of the impedance control to achieve the adaptive adjustment of the impedance control parameters. The contact force is obtained by the force/torque sensor, and

Table 1. Rules of fuzzy impedance parameter adjustment.

E\EC	NB	NM	NS	Z0	PS	PM	PB
NB	NB	NM	NS	Z0	Z0	Z0	Z0
NM	NB	NM	NS	Z0	Z0	Z0	PS
NS	NB	NS	NS	Z0	Z0	PS	PM
Z0	NB	NB	NS	Z0	PS	PB	PB
PS	NM	NS	Z0	Z0	PS	PM	PB
PM	NS	Z0	Z0	Z0	PS	PM	PB
PB	Z0	Z0	Z0	Z0	PS	PM	PB

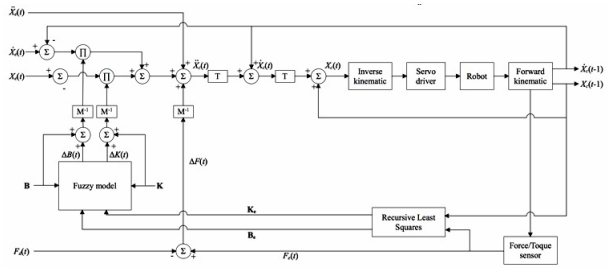

Fig. 2. The adaptive fuzzy impedance control schematic.

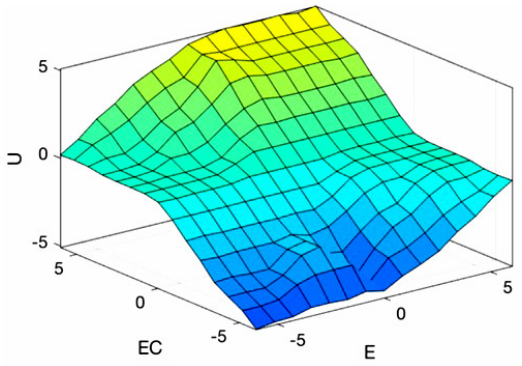

Fig. 3. The designed fuzzy rules.

the end effector position is calculated through the kinematics. The parameters of the environment are calculated by the contact force and the end effector position, and they are put into the fuzzy model to get the change value of the impedance parameters.

To make e_f = 0, the adaptive impedance used the fuzzy control [33, 34] as an online method in order to compensate the error of the estimation. To achieve this goal, the damping coefficient is used as an adaptive parameter to modify the impedance model. It is not recommended to set the inertia parameter because it is easy to cause system oscillation. If the range of the adjusted damping parameter b_d is Δb_d and the range of the adjusted stiffness parameter k_d is Δk_d [35], the rules of the fuzzy impedance parameter adjustment are given in Table 1 and the fuzzy rules are given in Fig. 3.

The impedance parameters b_d and k_d change under the fuzzy control when the interaction between the end-effector of the industrial robot and the environment occurs. After that, the

stiffness parameter k_d starts to approach to 0, because the desired error of force at the final is 0. The proposed method improves the performance of the force control while considering the environmental information.

4. Experiments

4.1 Experimental setup

To verify the feasibility of the adaptive impedance control algorithm, a 6-DOF independent developed industrial robot is used in the following experiments. The Denavit-Hartenberg (DH) parameters are calibrated by using the Leica Absolute Tracker AT960, and they are presented in Table 2.

In this industrial robot, the maximum payload is 4 Kg and the operation radius is 630 mm. In servo system, the motors in joints 1-3 are Panasonic MSMF042L1V2M and the motors in joints 4-6 are Panasonic MSMF012L1V2M. Also, the drivers in joints 1-3 are Panasonic MBDLN25BE and the drivers in joints 4-6 are Panasonic MADLN05BE. The controller of this robot is a Beckhoff industrial computer C6930 with the operating system Windows 10 and the communication bus EtherCAT. The software platform is TwinCAT3 and the PLC cycle time is 1 ms.

4.2 Sensitivity analysis

The sensitivities of the impedance parameters and the environmental stiffness are investigated, which determines the effect of different parameters on the performance of the force control.

The experiment for the constant force tracking is conducted on the plane, and the expected force is 20 N. The parameters of the impedance control and the environment are changed, respectively. As shown in Fig. 4(a), the environmental stiffness rises progressively from 10 to 100 and the remaining values are fixed. The manipulator's overshoot of the end contact force response curve as well as the reaction speed will steadily rise, and the steady-state error will continue to decrease. As shown in Fig. 4(b), the inertia parameter is increased from 1 to 50 and the other parameters are fixed. As the inertia parameters are increased, the overshoot of the end contact force response curve steadily increases, and the time required for the system to settle becomes longer, while the reaction speed is somewhat decreased. As shown in Fig. 4(c), the damping parameter is increased from 50 to 2000 and the other parameters are fixed. The overshoots of the response curves of the contact force and the speed rapidly diminish as the damping ratio increases. As shown in Fig. 4(d), the stiffness parameter is increased from 1 to 50 and the other parameters are fixed. The overshoot of the response curve of the contact force steadily diminishes as the stiffness parameter ratio increases, while the steady-state error increases and the response speed drops.

The preceding study demonstrates that adopting proper impedance settings for different environmental stiffnesses can improve the robot's force control performance. The sensitivity analysis, as shown in Fig. 4, provides a theoretical foundation of the adaptive parameter adjustment algorithms for robot force control, such as the fuzzy logic control or the neutrosophic logic/statistics.

Table 2. The DH parameters of 6-DoF industrial robot.

Joint	$\alpha_i\,(^\circ)$	$a_i\,(mm)$	$d_i\,(mm)$	$\theta_i\,(^\circ)$
1	90	29.90	379.50	0
2	0	270.60	0	90
3	90	69.27	0	0
4	–90	0	323.30	0
5	90	0	0	0
6	0	0	130.64	0

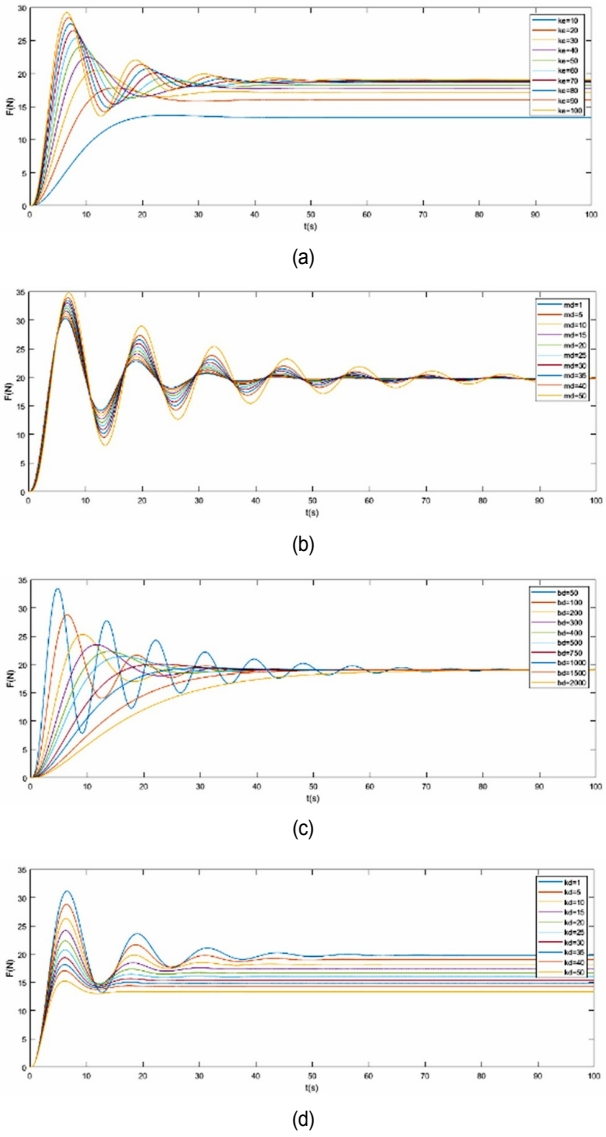

(a) (b) (c) (d)

Fig. 4. The sensitivity analysis on the contact force.

4.3 Simulation of the environmental parameter estimation

To illustrate the effectiveness of the online method of the environmental parameters estimation, the stiffness and the damping environmental parameters model is added to the impedance control system model in the simulation.

The simulation framework of the impedance control is built in Simulink to simulate the six-axis manipulator in the case of contact force interaction with the external environment. The environmental parameters are analyzed by collecting the value of contact force and the current displacement perpendicular to the contact surface.

As shown in Fig. 5, the simulation experiment of the environmental parameter estimation is designed to verify the algorithm. Considering the external environment with high rigidity in manufacturing, the environmental stiffness is set to be 10000 N/m and the environmental damping is set to be 0.1 Ns/m. For initial value setting in RLSA, the forgetting factor λ is set to be 0.9, the covariance matrix of the estimated parameters p (0) at the beginning time is set to be the identity matrix with size 2. The simulation time is 2 s and the fundamental sample time is set to be 1 ms, so the iterative operation is performed every one millisecond. The value represented by the blue line in Fig. 5 is the designed environmental value, and the purple line is the current iterative calculation value. It can be seen from Fig. 5 that in the first one hundred of iterations, the calculated value of the environmental stiffness quickly increases to the designed value. For the environmental stiffness, the estimated value reaches 90 % of the designed value after 80 iterations and it reaches 99 % of the designed value after 102 iterations. For the environmental damping, the estimated value reaches 90 % of the designed value after 42 iterations. Considering that the data tends to be stable after 0.1 s, the data between 0.1 s and 1 s are used for evaluation. The RMSE of the estimated environmental stiffness is 9.2324 N/m, and the MAPE of the estimated environmental stiffness is 0.0135 %. Also, the RMSE of the estimated environmental damping is 0.0033 Ns/m, and the MAPE of the estimated environmental damping is 1.388 %. Through the result of the simulation, it can be considered that after about 100 iterations of ILSM, the estimated environmental value can be regarded as the actual environmental value.

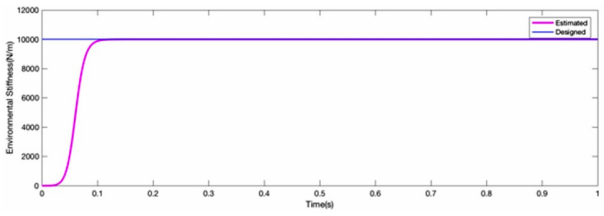

(a)

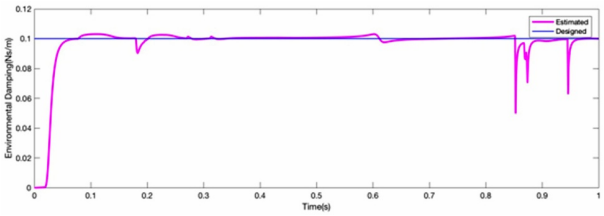

(b)

Fig. 5. The estimation of the environmental parameters.

4.4 Simulations of impedance control and adaptive fuzzy impedance control

First, the simulation for the constant force tracking is implemented on the plane, and the expected force is 15 N. For the impedance control, the inertia parameter is set as 1 Ns^2/m, the damping parameter is set as 500 Ns/m and the stiffness parameter is set as 50 N/m, respectively. The adaptive fuzzy impedance control is used for comparative experiment, also the damping parameter and the stiffness parameter in the impedance control are adjusted in real time. To illustrate the effectiveness of the proposed method, the conventional impedance control and the proposed adaptive fuzzy impedance control are compared. As shown in Fig. 6. The blue curve is the contact force controlled by the conventional impedance control, the red curve is the contact force controlled by the proposed adaptive fuzzy impedance control, and the black straight line is the expected contact force.

As shown in Fig. 6(a), the contact forces of the impedance control and the adaptive fuzzy impedance control both approach the desired force little steady-state error. The response time of the traditional impedance control is very long, and the contact force increases slowly in the process of contact with the plane. In contrast, the response time of the adaptive fuzzy impedance control is very fast. Within 0.5 s, the contact force increases rapidly to the desired force, and it has the overshoot about less than 0.5 N, which has a good contact force tracking effect.

Then, the simulation for the constant force tracking is conducted on the curved surface. The force tracking effect of the traditional constant impedance control is different from that of the previous plane constant force tracking, and the response speed is reduced. Although it can eventually become stable and close to the expected contact force, its response curve is very slow. At the beginning, the contact force increases slowly in the process of contact with the plane. In contrast, the response speed of the contact force response curve of adaptive impedance control has been significantly improved, and the expected contact force can be achieved in a shorer time, which has a better contact force tracking effect.

Next, the simulation for the constant force tracking is conducted under the variable environmental stiffness. As shown in Fig. 6(c), the expected force is 15 N. For the constant impedance controller, the inertia parameter is set to be 1 Ns^2/m, the damping parameter is set to be 500 Ns/m and the stiffness parameter is set to be 50 N/m, respectively. Under the condi-

tion of the variable environmental stiffness, the contact force overshoot of the constant parameter impedance control exceeds 160 N. At the same time, it takes 2 s for the system to enter the stable state, and the final steady-state error is about 15 N. In contrast, the overshoot of the fuzzy impedance control is about 2 N, the system enters a stable state after about 1 s, and the final steady-state error is about 1.5 N.

Finally, as the expected trajectory varies with time, the simulation for the constant force tracking is set up. As shown in Fig. 6(d), the constant force tracking simulation is carried out to make the expected force 15 N. For the constant impedance controller, other parameters are fixed as before. When the desired trajectory is changed, the contact force overshoot of the constant parameter impedance control is (about 0.2 N) larger than that of the fuzzy impedance control, and the steady-state error is (about 0.2 N) larger than that of the fuzzy impedance control.

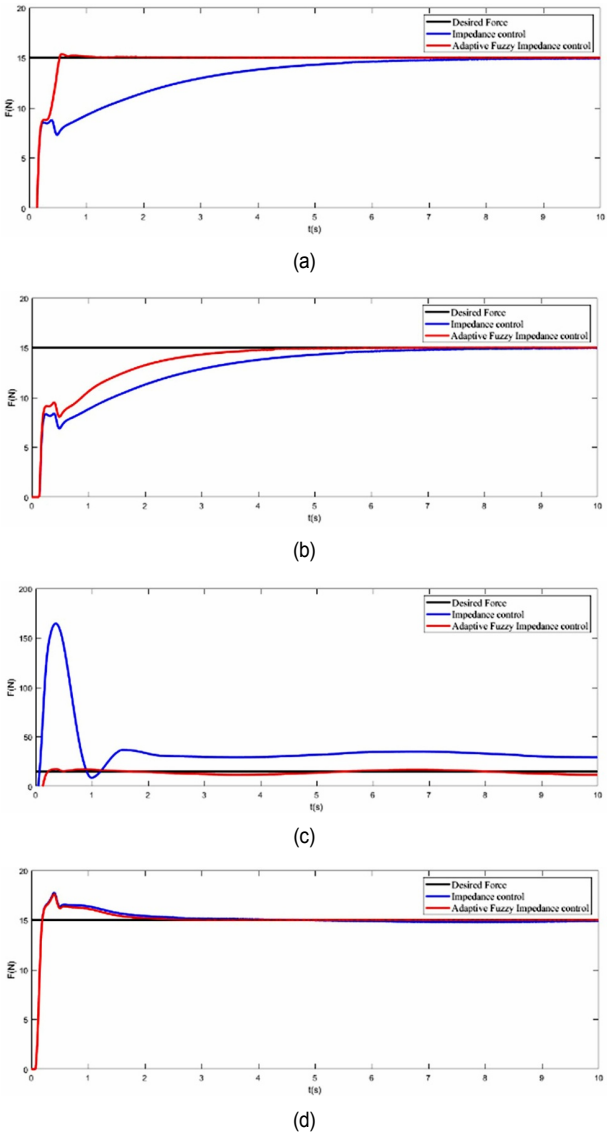

Fig. 6. Comparison between the impedance control and adaptive fuzzy impedance control.

4.5 Experiment of adaptive fuzzy impedance control in the plane

To verify the effectiveness of the proposed method, an experimental platform of robot polishing aluminum plates is built for verification. Fig. 7 shows the control framework of the adaptive fuzzy impedance algorithm. The equipment setups for the robot polishing are introduced as follows. The concentric rotary polishing machine in this article will rotate at high speed and produce strong vibrations. The vibration force of the polishing machine can be detected by the ATI six-dimensional force/torque sensor installed at the end of the robot. OPT-252 is used for polishing and grinding head. The displacement of the air compressor is 560 L/min and the maximum working pressure is 0.7 MPa. There are different specifications (P60-P2000) of sandpaper for grinding, and several specifications (W1.5-W60) related to the polishing paste for polishing.

The length of aluminum plate is 1000 mm, the width is 100 mm and the thickness is 3 mm. The material of aluminum plate is 6061 aluminum. The aluminum plate plane polishing process is shown in Figs. 8 and 9. The robot end effector approaches the aluminum plate in the position control mode. The robot then

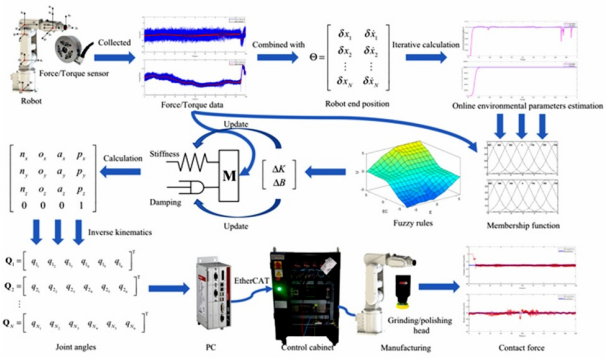

Fig. 7. The control structure of the adaptive fuzzy impedance model.

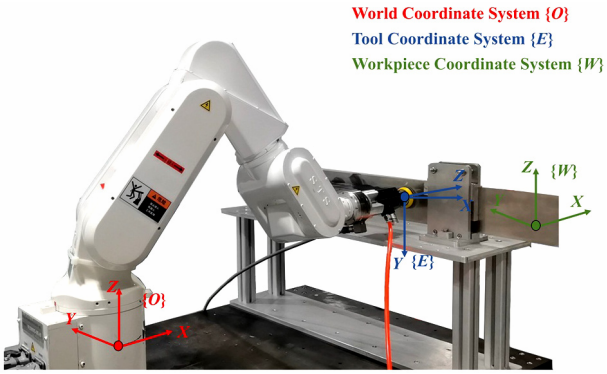

Fig. 8. Polishing of aluminum plate.

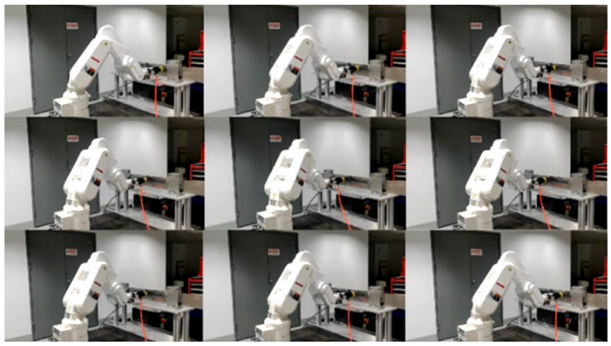

Fig. 9. Progress of polishing aluminum plate.

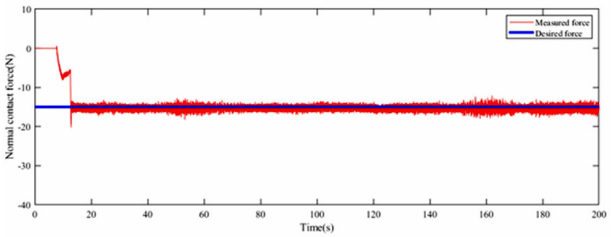

Fig. 10. Comparison of force tracking.

switches to the impedance control mode to contact the workpiece. The robot moves back and forth in a cycle of 200 s. The final contact force analysis is shown in Fig. 10. The blue line is the expected contact force 15 N and the red line is the constant force tracking. It can be seen from Fig. 10 that in the polishing experiment, there is almost no steady-state error, and the amplitude is about 2 N.

4.6 Experiment of adaptive fuzzy impedance control in curved surface

4.6.1 Normal constant force pose adjustment

The torque measured in the sensor coordinate system is **M**. Through the second-order system, the sensor coordinate system is obtained, and the angle correction to be adjusted is $\Delta\boldsymbol{\omega}$:

$$\Delta\boldsymbol{\omega} = \frac{1}{ms^2 + bs + k}\mathbf{M} . \tag{24}$$

To facilitate the solution of the robot inverse kinematic algorithm in the real-time controller, the pose adjustment in the end sensor's frame is converted to that in the base frame $\Delta\mathbf{W}$:

$$\Delta\mathbf{W} = \mathbf{R}\Delta\boldsymbol{\omega} \tag{25}$$

where $\mathbf{R}$ is the end pose before the adjustment.

The above pose adjustment $\Delta\mathbf{W}$ can be expressed in the form of axis angle $\theta\mathbf{r}$, where θ is the length of the vector and $\mathbf{r}$ is the unit direction vector. Substituting the antisymmetric matrix of the rotation vector $\mathbf{r}$ into the Rodrigues' rotation formula, the rotation matrix $\Delta\mathbf{R}$ of end pose correction can be written as:

$$\Delta\mathbf{R} = \begin{bmatrix} r_x^2(1-c\theta)+c\theta & r_x r_y(1-c\theta)-r_z s\theta & r_x r_z(1-c\theta)+r_y s\theta \\ r_x r_y(1-c\theta)+r_z s\theta & c\theta + r_y^2(1-c\theta) & r_y r_z(1-c\theta)-r_x s\theta \\ r_x r_z(1-c\theta)-r_y s\theta & r_y r_z(1-c\theta)+r_x s\theta & r_z^2(1-c\theta)+c\theta \end{bmatrix} \tag{26}$$

where $s\theta$ and $c\theta$ denote $\sin\theta$ and $\cos\theta$, respectively. Thus, after the adjustment, the following new end-effector pose is obtained:

$$\mathbf{T} = \begin{bmatrix} \Delta\mathbf{R}\cdot\mathbf{R} & \mathbf{p} \\ 0 & 1 \end{bmatrix} \tag{27}$$

where $\mathbf{p}$ is the end position before the adjustment. The new end-effector pose can be solved in the robot controller by the kinematic algorithm.

4.6.2 Grinding in the curved surface

To verify the effectiveness of the proposed method, an experimental platform for robotic grinding of the wind turbine blades is built. The selected workpiece is a wind turbine blade from a real wind turbine generator. The wind turbine blade is shown in Fig. 11. The length of the wind turbine blade is 1050 mm, the maximum thickness is 30 mm, and the minimum thickness is 10 mm. The material of wind turbine blade is glass fiber reinforced plastic. The selected workpiece and the experiment can verify the potential application of the proposed method in real industrial scenarios.

The experiment is carried out when the grinding head rotates. The information before and after filtering, and the end position collected by the six-dimensional force/torque sensor are plotted and analyzed. It can be seen from Fig. 12 that when the grinding head rotates and the grinding head contacts the curved surface, the vibrations in the *X* and *Y* directions will produce an amplitude of about 10 N. After filtering, the value of the contact force fluctuates slightly around 0 N. In the *Z* direction, the constant force tracking is carried out according to the value of the contact force. Before filtering, the amplitude 10 N of the contact force will affect the tracking accuracy and processing effect. After filtering, the force tracking effect can be significantly improved. If the vibrations of the measured torques along the *X* and *Y* directions in the tool coordinate system are too large, the robot pose adjustment cannot be controlled, and the filtered torque can meet the requirements of adjusting the pose. The positions along *X*, *Y* and *Z* directions in the workpiece coordinate system are analyzed. Due to the influence of force in *X* direction, it will be adjusted by the impedance controller. The adjusted information is shown in Fig. 12. It will move at a uniform speed in *Y* direction, maintain a constant value in normal direction, and conduct grinding experiment at the same height.

The overall diagram and the coordinate system of the experimental platform are shown in Fig. 13. The contact process

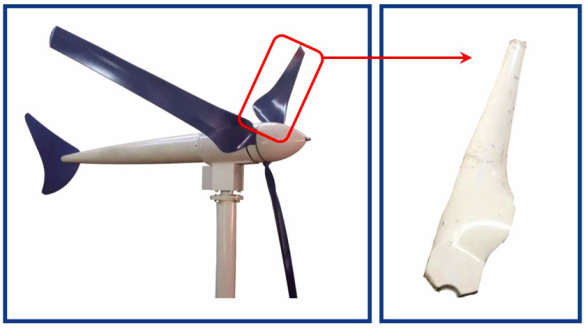

Fig. 11. The wind turbine blade workpiece.

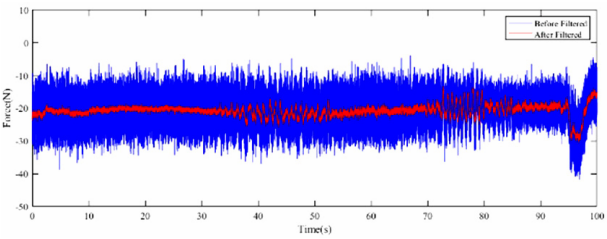

(a)

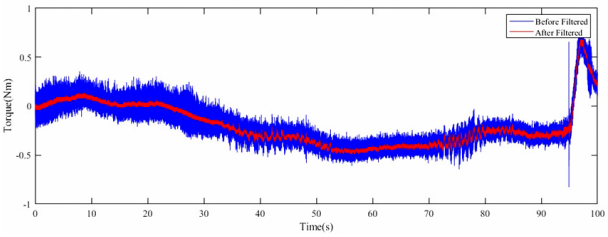

(b)

Fig. 12. Force/torque information when grinding.

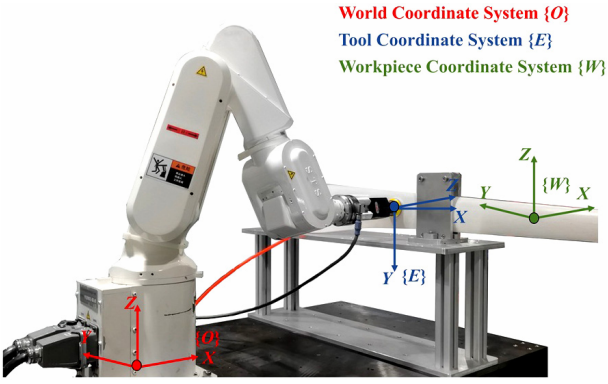

Fig. 13. Grinding of curved surface.

between the robot and the workpiece is introduced as follows. The robot end effector approaches the wind turbine workpiece in the position control mode. The robot then switches to the impedance control mode after contacting the workpiece. When the robot end effector contacts the workpiece, a large contact force is generated. The maximum value of the difference between the contact force and the desired force is the contact force overshoot. During the processing of contact, the improved impedance control algorithm mentioned above is applied to the grinding experiment with the robot adaptive pose adjustment according to the surface of wind turbine blade. Fig. 14 shows the grinding process of the curved surface. As shown in Fig. 15, the blue line is the desired contact force 20 N, and the red line is the normal contact force. The robot can adjust its pose in real time. The amplitude of the contact force is about 2 N, and the amplitude near the curvature is about 5 N, which has a good tracking effect.

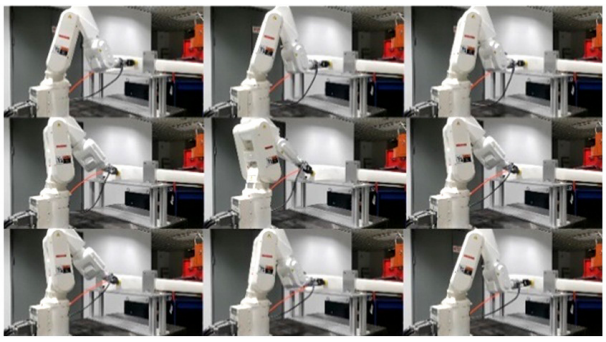

Fig. 14. Progress of grinding curved surface.

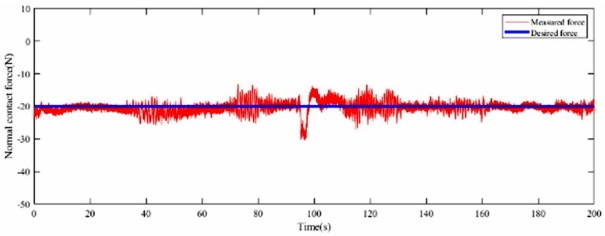

Fig. 15. Comparison of force tracking.

4.7 Discussion

Compared with the previous studies, this article combines the environmental parameters with the adjustments of the impedance parameters through the fuzzy logic controller and realizes the adaptive force control based on the estimated environmental information. This study makes up the weakness of previous works which only use the external force information and robot's position information when carrying out the adaptive constant force control under the condition of unknown or variable environmental parameters. In this article, the impedance parameters are adjusted more finely by the fuzzy logic control which contains the existing expert experience. Better performance of the adaptive force control can be achieved. The proposed algorithm can be applied to the robot constant force control under different environmental parameters with good environmental adaptability. It is verified by the robot polishing experiments and grinding experiments. The above experiments show that the adaptive fuzzy logic imped-

ance controller can achieve better performance with the oscillation below 2 N as the machining surface of the workpiece is not predefined.

The limitation of this study is that when the environment in contact with robot changes abruptly, the estimation of the environmental parameters cannot be quickly achieved and effectively converge to the true value. The adjustment of the impedance control parameters based on the real-time estimation will lag, which causes the steady-state error of the force control. In addition, the environmental stiffness model of this article is designed with less parameters to estimate the environmental status for real-time performance, which would reduce the accuracy of the environmental parameter estimation. The neutrosophic logic/statistics model [23-28] is a valuable option that can comprehensively and accurately describe the dynamic process of robot contact with environment, which would be combined with the current work as future research.

5. Conclusions

According to the traditional impedance control algorithm, a fuzzy-based impedance control algorithm is proposed. Through the actual experiment, the environmental stiffness estimation method is designed and verified for the external unknown stiffness environment. Due to the external environment information and the actual contact force information, the adjustment amount of the impedance parameters is obtained through the fuzzy controller to realize the variable impedance control. As the results of the simulations and actual experiments, it is concluded that the variable parameter mode of the fuzzy-based impedance control has significantly improved the force tracking accuracy and the environmental adaptability. The contact force error can be controlled within 2 N, which has a good effect. For the control algorithm mentioned above, it can be applied to the practical machining scenes such as grinding and polishing. Through the self-built robot force control platform, according to the adaptive impedance control framework, the grinding experiment of the aluminum plate and the polishing experiment of the wind turbine blade are carried out in the actual scenes. In terms of the collected force information, the adaptive variable impedance control algorithm has an obvious improvement in the constant force tracking compared with the traditional constant parameter impedance controller.

Acknowledgments

This work was supported in part by the NSFC-Shenzhen Robot Basic Research Center project U2013204.

References

[1] H. Zhou et al., A hybrid control strategy for grinding and polishing robot based on adaptive impedance control, *Adv. Mech. Eng.*, 13 (3) (2021) 1-21.

[2] H. Seraji and R. Colbaugh, Force tracking in impedance control, *Int. J. Robot. Res.*, 16 (1) (1997) 97-117.

[3] L. Roveda et al., Optimal impedance force-tracking control design with impact formulation for interaction tasks, *IEEE Robot. Autom. Lett.*, 1 (1) (2015) 130-136.

[4] X. Zhang and M. B. Khamesee, Adaptive force tracking control of a magnetically navigated microrobot in uncertain environment, *IEEE-ASME Trans. Mechatron.*, 22 (4) (2017) 1644-1651.

[5] J. Buchli et al., Learning variable impedance control, *Int. J. Robot. Res.*, 30 (7) (2011) 820-833.

[6] K. Kronander and A. Billard, Online learning of varying stiffness through physical human-robot interaction, *Proc. IEEE Int. Conf. Robot. Autom.*, Saint Paul (2012) 1842-1849.

[7] C. Passenberg, A. Peer and M. Buss, A survey of environment-, operator-, and task-adapted controllers for teleoperation systems, *Mechatronics*, 20 (7) (2010) 787-801.

[8] T. Tsuji and Y. Tanaka, On-line learning of robot arm impedance using neural networks, *Robot. Auton. Syst.*, 52 (4) (2005) 257-271.

[9] U. J. Na, A new impedance force control of a haptic teleoperation system for improved transparency, *J. Mech. Sci. Technol.*, 31 (12) (2017) 6005-6017.

[10] Y. Zhu and E. J. Barth, Impedance control of a pneumatic actuator for contact tasks, *Proc. IEEE Int. Conf. Robot. Autom.*, Barcelona (2005) 987-992.

[11] V. Panwar and N. Sukavanam, Design of optimal hybrid position/force controller for a robot manipulator using neural networks, *Math. Probl. Eng.*, 2007 (2007) 065028.

[12] H. Cao et al., Dynamic adaptive hybrid impedance control for dynamic contact force tracking in uncertain environments, *IEEE Access*, 7 (2019) 83162-83174.

[13] D. Surdilovic, Contact stability issues in position based impedance control: theory and experiments, *Proc. IEEE Int. Conf. Robot. Autom.*, Minneapolis (1996) 1675-1680.

[14] I. Bonilla et al., Path-tracking maneuvers with industrial robot manipulators using uncalibrated vision and impedance control, *IEEE Trans. Syst. Man Cybern. Part C-Appl. Rev.*, 42 (6) (2012) 1716-1729.

[15] G. Zeng and A. Hemami, An overview of robot force control, *Robotica*, 15 (5) (1997) 473-482.

[16] F. Nagata et al., Robotic sanding system for new designed furniture with free-formed surface, *Robot. Comput.-Integr. Manuf.*, 23 (4) (2007) 371-379.

[17] F. Domroes, C. Krewet and B. Kuhlenkoetter, Application and analysis of force control strategies to deburring and grinding, *Mod. Mech. Eng.*, 3 (6) (2013) 11-18.

[18] H. Kazerooni, J. J. Bausch and B. M. Kramer, An approach to automated deburring by robot manipulators, *J. Dyn. Sys., Meas., Control.*, 108 (4) (1986) 354-359.

[19] X. Wang, Y. Wang and Y. Xue, Adaptive control of robotic deburring process based on impedance control, *Proc. IEEE Intl. Conf. Ind. I.*, Singapore (2006) 921-925.

[20] F. Y. Hsu and L. C. Fu, Intelligent robot deburring using adaptive fuzzy hybrid position/force control, *IEEE Trans. Robot. Autom.*, 16 (4) (2000) 325-335.

[21] Z. Liu and Y. Sun, Adaptive variable impedance control with

fuzzy-PI compound controller for robot trimming system, *Arab. J. Sci. Eng.* (2022).
[22] Z. Li et al., A fuzzy adaptive admittance controller for force tracking in an uncertain contact environment, *IET Contr. Theory Appl.*, 15 (17) (2021) 2158-2170.
[23] M. Aslam, A new failure-censored reliability test using neutrosophic statistical interval method, *Int. J. Fuzzy Syst.*, 21 (4) (2019) 1214-1220.
[24] M. Aslam, Assessing the significance of relationship between metrology variables under indeterminacy, *MAPAN-J. Metrol. Soc. India.*, 37 (1) (2022) 119-124.
[25] M. Aslam, R. A. R Bantan and N. Khan, Design of a new attribute control chart under neutrosophic statistics, *Int. J. Fuzzy Syst.*, 21 (2) (2019) 433-440.
[26] M. Z. Khan et al., A fuzzy EWMA attribute control chart to monitor process mean, *Information*, 9 (12) (2018) 312-324.
[27] N. Jan et al., An approach towards decision making and shortest path problems using the concepts of interval-valued pythagorean fuzzy information, *Int. J. Intell. Syst.*, 34 (10) (2019) 2403-2428.
[28] Z. Khan et al., Neutrosophic rayleigh model with some basic characteristics and engineering applications, *IEEE Access*, 9 (2021) 71277-71283.
[29] E. Erickson, M. Weber and I. Sharf, Contact stiffness and damping estimation for robotic systems, *Int. J. Robot. Res.*, 22 (1) (2003) 41-57.
[30] J. Duan et al., Adaptive variable impedance control for dynamic contact force tracking in uncertain environment, *Robot. Auton. Syst.*, 102 (2018) 54-65.
[31] L. Marković et al., Adaptive stiffness estimation impedance control for achieving sustained contact in aerial manipulation, *Proc. IEEE Int. Conf. Robot. Autom.*, Xi'an (2021) 17-123.
[32] Z. X. Wang et al., Adaptive control strategy of robot polishing force based on position impedance, *Int. J. Mech. Mechatron. Eng.*, 15 (9) (2021) 427-433.
[33] P. Chen et al., Force control polishing device based on fuzzy adaptive impedance control, *Proc. Int. Conf. Lect. Notes. Artif. Int.*, 11743 (2019) 181-194.
[34] Z. Luo et al., Adaptive hybrid impedance control algorithm based on subsystem dynamics model for robot polishing, *Proc. Int. Conf. Lect. Notes. Artif. Int.*, 11745 (2019) 163-176.
[35] J. Yao et al., Cross-coupled fuzzy PID control combined with full decoupling compensation method for double cylinder servo control system, *J. Mech. Sci. Technol.*, 32 (5) (2018) 2261-2271.

Yichao Shen received the B.E. and M.E. degrees in Mechanical Engineering from Shanghai Jiao Tong University, Shanghai, China, in 2018 and 2021, respectively. His research interests include robotic force control machining, force control assembly of industrial robots, and robot machining path planning.

Yan Lu received the B.E. degree in Mechanical Engineering from Wuhan University of Technology, Wuhan, China, in 2019. He is currently pursuing a Ph.D. degree in Mechanical Engineering at Shanghai Jiao Tong University. His research interests include force control of industrial robots, vision based robotic grinding, and state monitoring of robot machining.

Chungang Zhuang received the Ph.D. degree from the School of Mechanical Engineering, Shanghai Jiao Tong University, Shanghai, China, in 2007. He is currently an Associate Professor with the School of Mechanical Engineering, Shanghai Jiao Tong University. His research interests include machine vision, force control of industrial robots, and multidisciplinary design and optimization.